Available online at www.sciencedirect.com
SCIENCE DIRECT®
PERGAMON
Polyhedron 22 (2003) 1951–1955
POLYHEDRON
www.elsevier.com/locate/poly

Examining the thermolysis reactions of nanoscopic Mn_{12} single molecule magnets

Philippe Gerbier [a,*], Daniel Ruiz-Molina [b,*], Jordi Gómez [b], Klaus Wurst [c], Jaume Veciana [b]

[a] UMR 5637, Université Montpellier 2, C.C.007, Place E. Bataillon, 34095 Montpellier, France
[b] Institut de Ciència de Materials de Barcelona (CSIC), Campus UAB, 08193 Cerdanyola, Spain
[c] Anorganische und Theorische Chemie, Universität Innsbruck, Innrain 52a, A-6020, Innsbruck, Austria

Received 6 October 2002; accepted 28 October 2002

Abstract

The thermal behavior of three Mn_{12} single molecule magnets $[Mn_{12}O_{12}(O_2CC_6H_5)_{16}(H_2O)_4]\cdot CH_2Cl_2\cdot C_6H_5CO_2H$ (**1**), $[Mn_{12}O_{12}(O_2C^tBu)_{16}(H_2O)_4]$ (**2**) and $[Mn_{12}O_{12}(O_2CCHCl_2)_{16}(H_2O)_4]$ (**3**) is reported. Aromatic ligands allow the complex **1** to be stable up to 300 °C whereas alkyl groups decrease drastically the domain of thermal stability for the complexes **2** and **3**. Moreover, the thermal decarboxylation of complexes **2** and **3** generates $[Mn_6O_2(O_2CR)_{10}L_4]$ (L = H_2O, HO_2CR) complexes as characterized by single crystal X-ray diffraction when R = ^{t}Bu.

Keywords: Mn_{12}; Single molecule magnets; Thermal stability; Thermolytic synthetic methods

1. Introduction

The use of synthetic methodologies, the so-called *bottom-up approach*, offers a potential alternative to obtain monodispersed nanoscale magnetic materials of a sharply defined size. In this order, the discovery of large metal cluster complexes with interesting magnetic properties characteristic of nanoscale magnetic particles, such as out-of-phase ac magnetic susceptibility signals and stepwise magnetization hysteresis loops, represented an important discovery to access ultimate high-density information storage devices and quantum computing applications [1]. Moreover, such clusters are composed of a single and sharply defined size and are agreeable to variations in peripheral carboxylate ligation making them soluble in different solvents. Different families of complexes that function as single molecule magnets (SMMs) based on manganese [2], nickel [3], cobalt [4] iron [5] and mixtures of metals [6] have been obtained. However, even though different families of SMMs have been synthesized (vide supra), all of them show low blocking temperatures (T_B) above which they behave as superparamagnets. One of the highest T_B ($\approx$6 K) so far reported corresponds to the Mn_{12} family. These complexes possess a $[Mn_{12}(\mu_3\text{-}O)_{12}]$ core comprising a central $[Mn_4^{IV}O_4]^{8+}$ cubane held within a non-planar ring of eight Mn^{III} ions by eight μ_3-O^{2-} ions. Peripheral ligation is provided by sixteen carboxylate groups and three or four H_2O ligands [7]. Since the above discoveries, the interest to obtain new SMMs with larger dimensionalities, anisotropies and high-spin ground states has grown considerably and for this reason different chemical synthetic methods to obtain new SMM with higher T_B are being widely explored worldwide.

In our group, the motivating physical work has been the exploration of new synthetic methods to obtain nanoscale clusters via thermolysis reaction. More precisely, in this work we have explored the thermal

* Corresponding authors. Fax: +34-935-805-729 (D.R.); +33-4-67-14-38-52 (Ph.G.).
E-mail addresses: gerbier@univ-montp2.fr (P. Gerbier), dani@icmab.es (D. Ruiz-Molina).

0277-5387/03/$ - see front matter
doi:10.1016/S0277-5387(03)00158-X

behavior of three different Mn_{12} SMM: $[Mn_{12}O_{12}(O_2CC_6H_5)_{16}(H_2O)_4]\cdot CH_2Cl_2\cdot C_6H_5CO_2H$ (**1**), $[Mn_{12}O_{12}(O_2C^tBu)_{16}(H_2O)_4]$ (**2**) and $[Mn_{12}O_{12}(O_2CCHCl_2)_{16}(H_2O)_4]$ (**3**). We will show how the different carboxylate ligands of complexes **1–3** influence their thermal stability. In this order, the thermal treatment of complexes **2** and **3** toluene yields the lower nuclearity Mn_6 clusters, whereas complex **1** remains thermally stable without any side-decomposition reaction.

2. Experimental

All the reagents were used as received. Microanalyses were performed by the Servei d'Analisi of the Universitat de Barcelona. $[Mn_{12}O_{12}(O_2CC_6H_5)_{16}(H_2O)_4]\cdot CH_2Cl_2\cdot C_6H_5CO_2H$ (**1**) [8], $[Mn_{12}O_{12}(O_2C^tBu)_{16}(H_2O)_4]$ (**2**) [9] and $[Mn_{12}O_{12}(O_2CCHCl_2)_{16}(H_2O)_4]$ (**3**) [10] were prepared following the methodology previously described. Dc magnetic measurements were carried out on a Quantum Design MPMS SQUID magnetometer equipped with a 5.5 T magnet in the temperature range of 1.8–300 K. Pascal's constants were used to subtract the diamagnetic contribution of the substances analyzed. Simultaneous TG/DTA measurements were performed under an N_2+O_2 flow (60 ml min^{-1}) at a heating rate of 5 °C min^{-1} on a Setaram Labsys TG-TDA12 thermogravimetric analyzer.

2.1. X-ray crystallography

X-ray data were collected at 223 K, on a Kappa CCD diffractometer with monochromatic Mo Kα ($\lambda =$ 0.71073 Å) radiation. Data were collected via ϕ- and ω-multiscans and reduced with the program DENZO-SMN without absorption correction. The structure was refined by a full-matrix least-squares method (Table 1).

2.2. $[Mn_6O_2(O_2C^tBu)_{10}(C_3H_4N_2)_4]\cdot C_6H_5CH_3$ (4)

A solution of complex **2** (1.00 g, 0.4 mmol) in toluene (20 ml) was refluxed for 24 h. To the cooled solution was added pyrazole (0.60 g, 8.8 mmol) and the mixture was heated in order the help the dissolution of the solids. The filtered solution was left undisturbed overnight at room temperature in an open Erlenmeyer flask to afford X-ray quality diamond-shaped crystals (0.94 g, 65%). FTIR (KBr, cm^{-1}): 3333 (medium, NH str); 2958 (medium, C–H str); 1587, 1570, 1482, 1416 (strong, CO_2^- str); 1430 (weak, ^{t}Bu bend). Elemental analysis Calcd for $C_{69}H_{114}N_8O_{22}Mn_6$: C 47.70, H 6.57, N 6.45. Found: C 47.59, H 6.52, N 5.96%.

Table 1
Crystallographic data for $[Mn_6O_2(O_2C^tBu)_{10}(C_3H_4N_2)_4]\cdot C_6H_5CH_3$ (**4**)

Parameter	Complex **4**
Formula	$C_{69}\ H_{110}\ Mn_6\ N_8\ O_{22}$
Formula wt. (g mol^{-1} [a])	1733.29
Crystal system	Orthorhombic
Space group	*Pbcn*
a (Å)	14.1338(3)
b (Å)	22.9458(4)
c (Å)	27.0464(3)
α (°)	90
β (°)	90
γ (°)	90
V (Å^3)	8771.5 (3)
Z	4
T (K)	223(2)
Crystal size (mm)	$0.35\times0.30\times0.15$
Radiation l (Å [b])	0.71073
ρ_{calc} (g cm^{-3})	1.313
Data collected	$1\le 2\theta\le 24$
$R(R_w)$ [c]	0.0389(0.0557)

$f_{gof}=[\Sigma w(|F_o|-|F_c|)^2]/(n-p)]^{1/2}$; $n=$ observed reflections, $p=$ refined parameters. [c] $F>3\sigma(F)$.

[a] Including solvent molecules.

[b] Graphite monochromator.

[c] $R=\Sigma F_o|-|F_c||/\Sigma|F_o|$. $R_w=[\Sigma w(|F_o|-|F_c|)^2]^{1/2}$, where $w=1/s^2|F_o|$.

3. Results and discussion

3.1. Thermal stability: TGA/DTA experiments

Thermogravimetric analyses (TGA) combined with differential thermal analyses (DTA) were carried out on complex **1** and **2**. At the first glance, the TG curves (Fig. 1) seem to indicate a marked difference between their thermal stabilities, complex **1** being more stable at higher temperatures.

Both complexes exhibit a weight loss in the temperature range of 70–140 °C that has been attributed to the elimination of 4 H_2O+1 CH_2Cl_2 (obs.: 5.9%, th.: 4.7%) for complex **1** and 4 H_2O+1 $^tBuCO_2H$ (obs.: 7.0%, th.: 6.8%) for complex **2**. An increase of the temperature evidenced that complex **1** remained stable at least up to 210 °C where an additional weight loss of approximately 5% was observed ($-C_6H_5CO_2H=4\%$). A further increase of the temperature yields the final exothermal degradation with an overall weight loss of 67.4%. On the contrary, complex **2** is stable up to 150 °C, whereupon it underwent an impressive thermal degradation as ascertained by an abrupt two-step weight loss (48.2%) associated to a broad intense exothermal peak in the DTA curve.

Where does the different thermal stability of complexes **1** and **2** arise from? One of the most reasonable answer is that this difference may arise from electronic effects afforded by the organic group attached to the carboxylate moieties, and therefore to the acidity of

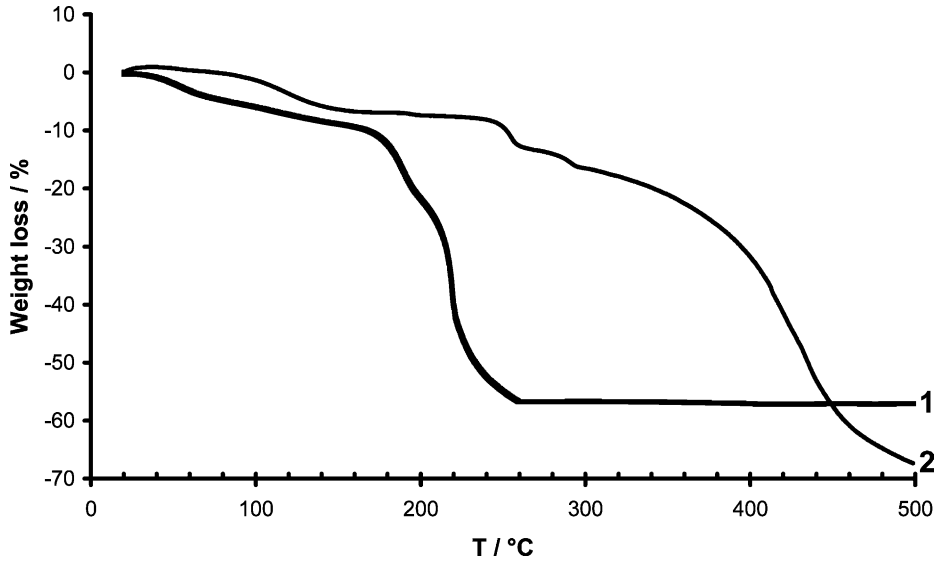

Fig. 1. TGA of complexes **1** and **2** under an air flow.

their associated protonated form. On the other hand steric considerations of the peripheral ligands may be also of interest to explain this observation. To give more insight into the origin of the different thermal stabilities, DTA experiments were carried out over a polycrystalline sample of complex **3**. The $-CHCl_2$ group has similar dimensions than the ^{t}Bu group although its acidity is higher due to the presence of the chlorine atoms. The DTA curves of complex **3** indicated that it becomes thermally unstable over 110 °C as ascertained by a broad intense exothermal peak and by IR spectroscopy. The IR spectra of a polycrystalline sample of complex **3** treated at four different temperatures are shown in Fig. 2. As can be seen there, at temperatures above 110 °C the different patterns of absorption experience considerable variations, indicating that decomposition side reactions take place. This fact seems to indicate that both, the steric compression afforded by bulky carboxylic groups and their different acidic character influence the relative thermal stability of Mn_{12} complexes.

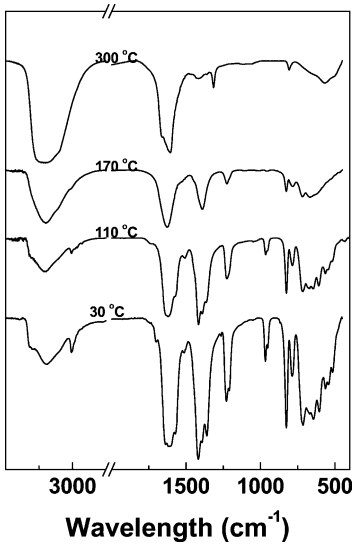

Fig. 2. Infrared spectra of complex **3** recorded in KBr after thermal treatments at 30, 110, 170 and 300 °C.

3.2. Mass spectrometry

The mass spectra of complexes **1–3** have been recorded. Since the Mn_{12} clusters absorb at the wavelength of the laser light used in the TOF MS instrument, mass spectra were recorded both with and without a matrix under different experimental conditions [11]. In the case of complex **1**, the high mass region (>700 Da) LDI-TOF mass spectrum recorded in positive mode, reveals no peak corresponding to the molecular ion but does show a series of peaks corresponding to the $[Mn_{12}O_{12}(O_2CC_6H_5)_{14}]^+$ ion at $m/z \sim 2547$ and fragments of it resulting from the stepwise loss of several $C_6H_5CO_2$ units ($\Delta m/z \sim 121$). In the low-mass region of the spectrum (<700 Da) a series of peaks, which could not be directly assigned to fragmentations involving the presence of the benzoate anion, are observed. These fragments may arise from rearrangement of the original cluster, and their explanation must involve the presence of manganese, oxygen and carbon atoms. Finally, it has to be emphasized that the benzoate complex **1** yielded good quality mass spectra independently of the matrix and polarity used.

The MALDI-TOF MS mass spectrum of complex **2** in the positive mode using 2-amino-4-methyl-5-nitropyridine (AMNP) as a matrix exhibits the most abundant pseudo-molecular peak was observed at $m/z = 2065$ [M-$4H_2O$-4^tBuCO_2]$^+$. In addition to such peak, an intense pattern centered at about $m/z = 1475$, which was not

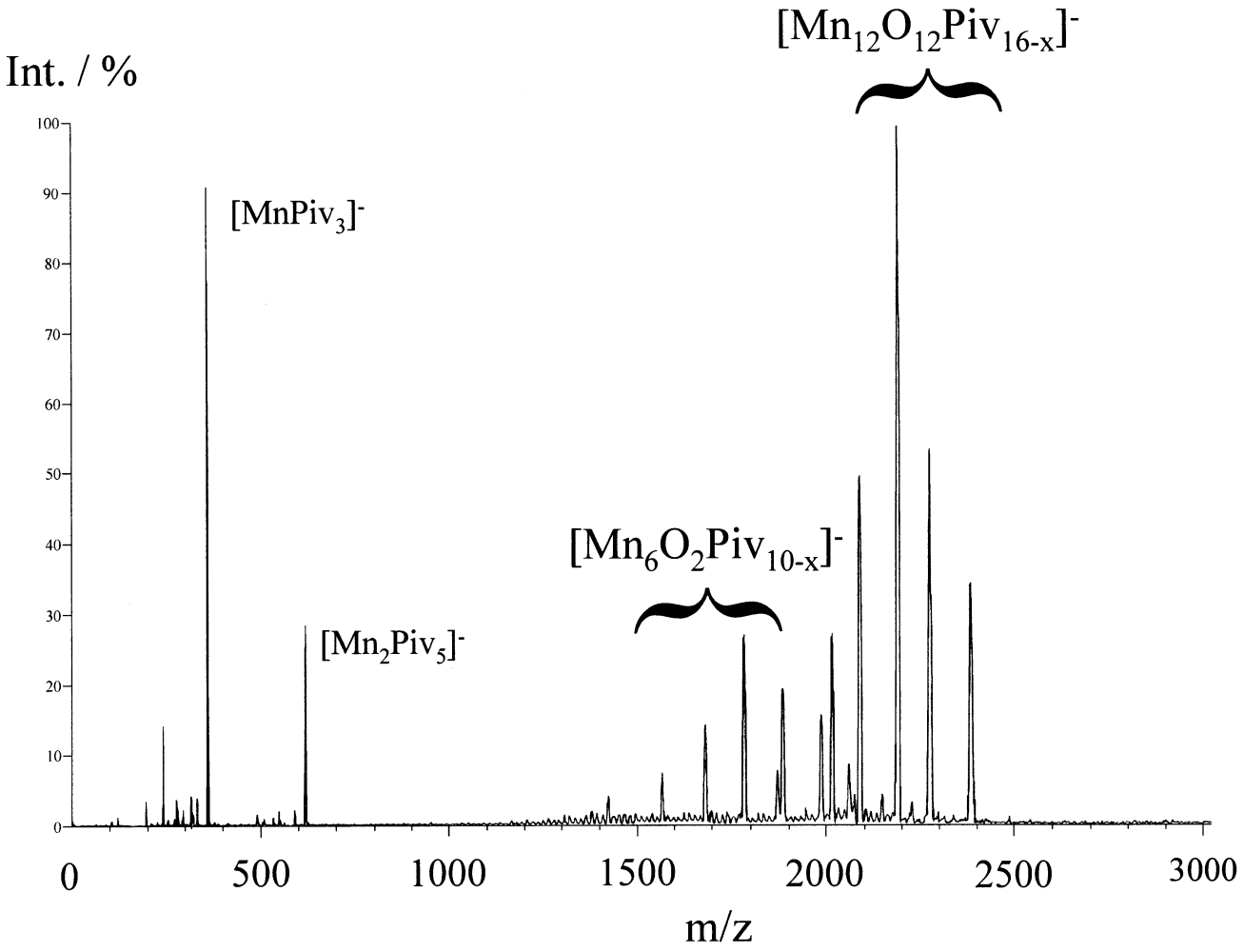

Fig. 3. Negative-ion mode MALDI-TOF spectrum of complex **2** using AMNP as a matrix.

observed for complex **1**, appears (Fig. 3). Since most of the peaks are related each other by the gain or the loss of a pivalate ($m/z = 101$) ligand, this spectral zone should be attributed to a family of mixed ligand complexes derived from the already known mixed valence Mn(II, III) complexes $[Mn_6O_2(O_2C^tBu)_{10}L_4]$ [12].

3.3. Thermolysis reaction

A toluene solution of **2** was refluxed for 24 h. On cooling, a red–brown microcrystalline precipitate was obtained. Such precipitate was characterized as an incompletely coordinated $[Mn_6O_2(O_2C^tBu)_{10}L_4]$ (L = H_2O, $^tBuCO_2H$) complex by comparison with the IR spectra of related Mn_6 complexes prepared as previously described in the literature. [13] This fact, together with previous mass spectrometry experiments, seems to indicate that in a first step, some of the Mn^{III} and Mn^{IV} ions constitutive of the starting complex are reduced to Mn^{II} ions by an oxidative decarboxylation mechanism of the ligands (Eq. (2)) [14].

$$[Mn_{12}^{(III,IV)}O_{12}(O_2C^tBu)_{16}(H_2O)_4] \rightarrow [Mn^{II}(O_2C^tBu)_2(H_2O)_x] + {}^t Bu^{\bullet} + CO_2 + H_2O + \ldots \quad (2)$$

Most likely, in a second step, the aggregation–dehydration reaction of the so-formed Mn^{II} pivalates lead to the hexamanganese mixed valence complexes according to Eq. (3) where L = H_2O, $^tBuCO_2H$.

$$6[Mn^{II}(O_2C^tBu)_2(H_2O)_x] \rightarrow [Mn_6^{(II,III)}O_2(O_2C^tBu)_{10}L_4] \quad (3)$$

Such ligands were subsequently replaced by reaction with pyrazole ligands. Indeed, addition of pyrazole to a warm mixture of $[Mn_6O_2(O_2C^tBu)_{10}L_4]$ and posterior cooling of the solution yielded nice brown diamond-shaped crystals of $[Mn_6O_2(O_2C^tBu)_{10}(C_3H_4N_2)_4]\cdot C_6H_5CH_3$ (**4**) suitable for X-ray structure determination. The ORTEP plot of complex **4** is shown in Fig. 4. The structure is similar to those previously found for related Mn_6 consisting of an edge-sharing bitetrahedral cage bridged by two μ_4-oxides and a mixture of six 1,3- and

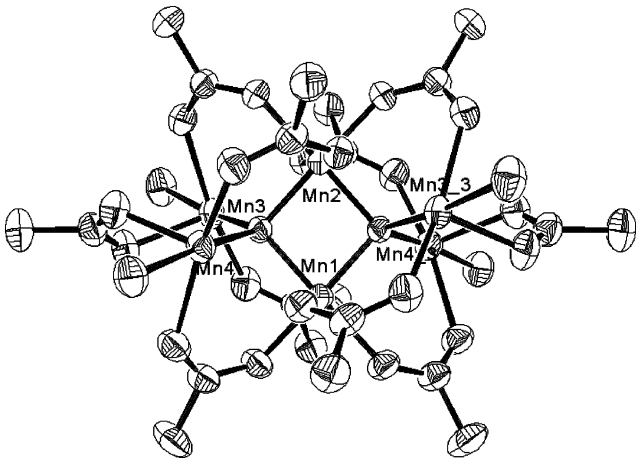

Fig. 4. ORTEP drawing of the Mn_6 core of complex **4** with thermal ellipsoids at 50% of probability. The hydrogen atoms and the organic peripheral groups were omitted for clarity.

four 1,1,3- pivalate ligands. The four pyrazole ligands are bound to the wing-tip sites of the manganese octahedrons. Magnetic measurements carried out on complex **4**, showed an antiferromagnetic coupling of the manganese ions leading to a $S = 0$ ground state as exactly observed with other related complexes.

Finally it has to be emphasized that thermal treatment of a toluene solution of **3** yielded a related $[Mn_6O_2(O_2CCHCl_2)_{10}L_4]$ ($L = H_2O$, HO_2CCHCl_2) complex as ascertained by different spectroscopic techniques and magnetic measurements. However, despite recurrent diffusion and crystallization experiments, the obtaining of single crystals of enough quality to solve its X-ray structure remained elusive. On the other side, similar thermal studies over a toluene solution of complex **1** revealed that it remains stable over several hours, even days. Such results are in agreement with the larger stability of complex **1** when compared to complexes **2** and **3** as ascertained by TG/DTA experiments and the lack of peaks associated to clusters with reduced dimensionalities in its MALDI-TOF spectra.

4. Conclusion

The thermolytic studies of Mn_{12}-based SMMs have shown that their thermal stability was highly dependent of parameters such as the electron-withdrawing ability and the bulkiness of the peripheral organic groups. The thermal degradation of SMM with non-aromatic groups follows an oxidative decarboxylation of the ligands by the Mn^{III} and Mn^{IV} ions which generates Mn^{II} ions, carbon dioxide and an organic radical. Interestingly, the thermal decarboxylation of SMM is found to open new synthetic methods to prepare others manganese clusters upon a thermal treatment.

4.1. Supplementary material

Complete lists with atomic coordinates, anisotropic displacement parameters, bond lengths and angles have been deposited at the Cambridge Crystallographic Data Centre (CCDC No. 195546), 12 Union Road, Cambridge, CB2 1EZ, UK (fax: +44-1223-336033; e-mail: deposit@ccdc.cam.ac.uk or www: http://www.ccdc.cam.ac.uk).

Acknowledgements

This work was supported from DGI (MAT 2002-00433), DGI (MAT 2000-1388-C03-01) and the 3MD Network of the TMR program of the E.U. (contract ERBFMRXCT 980181). Ph.G. is grateful to the CSIC and to the Région Languedoc-Roussillon for their financial support.

References

[1] G. Christou, D. Gatteschi, D.N. Hendrickson, R. Sessoli, MRS Bull. 25 (2000) 56.
[2] C. Boskovic, W. Wernsdorfer, K. Folting, J.C. Huffman, D.N. Hendrickson, G. Christou, Inorg. Chem. 41 (2002) 5107 (and referenced cited therein).
[3] C. Cadiou, M. Murrie, C. Paulsen, V. Villar, W. Wernsdorfer, R.E.P. Winpenny, Chem. Commun. 24 (2001) 2666.
[4] E.C. Yang, D.N. Hendrickson, W. Wernsdorfer, M. Nakano, G. Christou, J. Appl. Phys. 91 (2002) 7382.
[5] (a) C. Sangregorio, T. Ohm, C. Paulsen, R. Sessoli, D. Gatteschi, Phys. Rev. Lett. 78 (1997) 4645.;
(b) A.L. Barra, A. Caneschi, A. Cornia, F.F. De Biani, D. Gatteschi, C. Sangregorio, R. Sessoli, L. Sorace, J. Am. Chem. Soc. 121 (1999) 5302.
[6] J.J. Sokol, A.G. Hee, J.R. Long, J. Am. Chem. Soc. 124 (2002) 7656.
[7] D. Ruiz-Molina, G. Christou, D.N. Hendrickson, Mol. Cryst. Liq. Cryst. 343 (2000) 17.
[8] R. Sessoli, H.-L. Tsai, A.R. Schake, S. Wang, J.B. Vincent, K. Folting, D. Gatteschi, G. Christou, D.N. Hendrickson, J. Am. Chem. Soc. 115 (1993) 1804.
[9] Ph. Gerbier, D. Ruiz-Molina, N. Domingo, D.B. Amabilino, J. Vidal-Gancedo, J. Tejada, D.N. Hendrickson, J. Veciana, Monatsch, Chem.134 (2003) 265.
[10] M. Soler, P. Artus, K. Folting, J.C. Huffman, D.N. Hendrickson, G. Christou, Inorg. Chem. 40 (2001) 4902.
[11] D. Ruiz-Molina, Ph. Gerbier, E. Rumberger, D.B. Amabilino, I.A. Guzei, K. Folting, J.C. Huffman, A. Rheingold, G. Christou, J. Veciana, D.N. Hendrickson, J. Mater. Chem. 12 (2002) 1152.
[12] A.R. Schake, J.B. Vincent, Q. Li, P.D.W. Boyd, K. Folting, J.C. Huffman, D.N. Hendrickson, G. Christou, Inorg. Chem. 28 (1989) 1915.
[13] (a) M. Murrie, S. Parsons, R.E.P. Winpenny, J. Chem. Soc., Dalton Trans. 1 (1998) 1423;
(b) A.R.E. Baikie, A.J. Howes, M.B. Hursthouse, A.B. Quick, P. Thornton, J. Chem. Soc., Chem. Commun. (1986) 1587;
(c) A.S. Batsanov, Yu.T. Struchkov, G.A. Timko, N.V. Gerbeleu, O.S. Manole, S.V. Grebenko, Koord. Khim. 20 (1994) 604.
[14] J.M. Anderson, J.K. Kochi, J. Am. Chem. Soc. 92 (1970) 2450.